MICROSTRUCTURE AND DEFORMATION RESISTANCE IN ROLLING OF ALUMINIUM FOIL

H. ABRAL*, J. KROC*,, W. BLUM* and J. HIRSCH*****

* Inst. f. Werkstoffwissenschaften, LS I, Martensstraße 5, D-91058 Erlangen, Germany
** on leave from Dep. of Metal Physics, Charles University, Ke Karlovu 5, 121 16 Praha 2, Czech Republic
*** VAW aluminium AG, Postfach 2468, D-53014 BONN, Germany

ABSTRACT Transmission electron microscopic observations of technically pure Al (AA 1050) show that the grain structure approaches a steady state during foil rolling due to dynamic recovery and geometric dynamic recrystallization. It is characterized by pancake shaped subgrains of 0.45 μm thickness and an aspect ratio of 0.5 in flat grain layers of 1 μm thickness. As a result of microstructural evolution the tensile strength of the foils remains approximately constant with increasing rolling strain. The evolution of deformation resistance and microstructure can be simulated with a simple model using the dislocation density as single microstructural parameter.

Keywords: *AA 1050, foil rolling, geometric dynamic recrystallization, distribution of grain misorientation, deformation kinetics, structure evolution*

1. INTRODUCTION

Rolling of thin foil is a highly sophisticated process in which the material deforming at high speed between the rolls plays an important part. In the present work attention is focussed on the microstructure and the deformation kinetics of pure Al under conditions of rolling. The results are described by a simple model of deformation during rolling.

2. EXPERIMENTAL DETAILS

Rolling started from a sheet of Al of commercial purity (AA1050) of 699 μm thickness with a grain size $d_0 = (20.4 \pm 0.7)$ μm. It was rolled in 6 passes to a final thickness of 6.5 μm. The microstructure was investigated by transmission electron microscopy (TEM) of thin sections with normals parallel to the directions indicated in Fig. 1 (in the following abbreviated as X-sections with normals X = N, T, R). The T- and R-sections were prepared by a special stacking technique [1]. Fig. 2 shows a detail from a T-section of a rolled foil. All boundaries are visible in TEM independent of their misorientation. The misorientations of boundaries (minimum angles Ψ of rotation to coincidence) were evaluated from the orientations of the neighbouring crystals determined from Kikuchi line patterns at positions close to the boundaries (Fig. 2) with the software of Voigt [2]. Subgrain sizes w_{XY} and grain sizes d_{XY} were determined as spacings of all and of large angle boundaries ($\Psi > 15°$), respectively, along a test line in X-direction in a Y-section. Fast compression tests at constant true strain rate $\dot{\epsilon}$ (up to 100/s) were performed at the Institut für Bildsame Formgebung of the RWTH Aachen (Germany) on specimens of 30 mm height and 20 mm diameter. Sections for TEM were taken from the center of the specimens.

3. RESULTS

3.1 Microstructure

From the Ψ-distributions in Fig. 3 it is seen that the fraction of small angle boundaries ($\Psi < 15°$) in the T-plane decreases from ≈ 0.8 at the true compressive strain $\epsilon = 1.5$ to ≈ 0.3 at $\epsilon = 4.7$, i.e. the majority of boundaries found in the T-plane after rolling to $\epsilon = 4.7$ (cor-

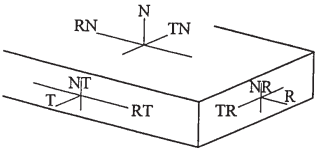

Figure 1: N: normal direction of rolled foil, R: rolling direction, T: transverse direction, RN: rolling direction in section perpendicular to N etc.

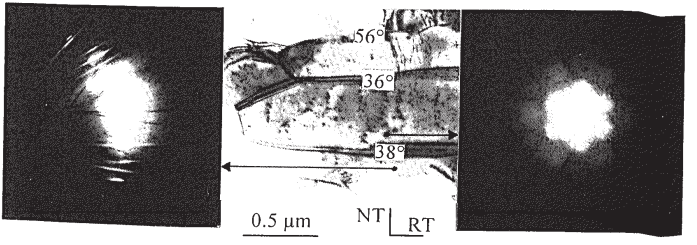

Figure 2: TEM picture of T-section after rolling ($\epsilon = 4.7$). Numbers indicate angles of misorientation. Two Kikuchi line patterns are shown for example.

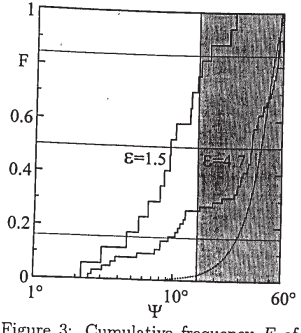

Figure 3: Cumulative frequency F of boundary misorientations Ψ measured in T-sections after rolling to $\epsilon = 1.5$ and 4.7. Dotted curve: statistical grain orientation.

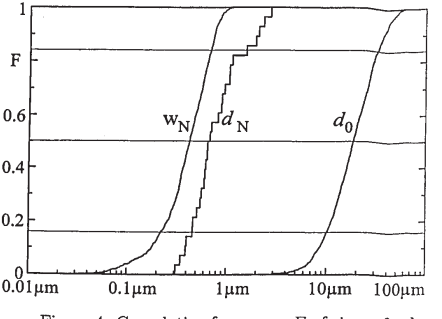

Figure 4: Cumulative frequency F of sizes of subgrains and grains measured in N-direction after rolling to $\epsilon = 4.7$. d_0 denotes initial grain size distribution.

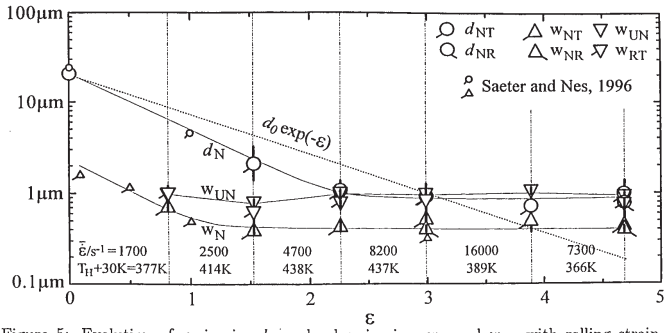

Figure 5: Evolution of grain size d_N and subgrain sizes w_N and w_{UN} with rolling strain ϵ. Vertical lines mark ends of rolling passes. Small symbols from [3].

responding to 6.5 μm foil thickness) are large angle boundaries. Fig. 4 gives the distributions of subgrain and grain sizes in N-direction after rolling to $\epsilon = 4.7$. As expected there are no significant differences between the data measured in T- and R-planes. The d_N-values are shifted from the w_N to the right by a factor < 2. This means that the fraction of small angle boundaries measured in N-direction is less than 0.5, consistent with Fig. 3.

Fig. 5 displays the variation of the average sizes of subgrains and grains with rolling strain ϵ. Starting from the initial grain size d_0 one expects d_N to decrease according to the dotted line. For $\epsilon < 3$, however, the actual decrease is stronger than expected. This is attributed to the fact that the grain boundaries get serrated and that low angle boundaries develop into large angle boundaries [3,4]. Beyond $\epsilon = 2.5$, however, d_T ceases to decrease. This means that the continuous increase of large angle boundary area during compression is compensated by recombination of boundaries [5,6]. The subgrain size w_{UN}, measured in unspecified directions in N-sections where the subgrains appear equiaxed, remains fairly constant with ϵ. w_N [1] saturates at $\epsilon \approx 1.5$. It is smaller than the subgrain size w_{UN} measured in the rolling plane; the aspect ratio is $w_N/w_{UN} \approx 0.5$.

After uniaxial compression at 300 K and constant $\dot{\epsilon}$ to $\epsilon \approx 0.69$, w_{UN} was found to be a unique function of the normal stress σ normalized by the shear modulus $G(T)$ [7]:

$$w_{UN} = k_w \, b \, G/\sigma \qquad k_w = 18 \tag{1}$$

($b = 0.286$ nm: length of Burgers vector). The subgrain aspect ratio in uniaxial compression is in the same order as in rolling. The steady state flow stress was determined from $d\sigma/d\epsilon$-σ-curves by by extrapolation to $d\sigma/d\epsilon = 0$. Fig. 6 displays the data in normalized coordinates.

4. ANALYSIS

The present observations show that the grain structure attains a quasi steady state during rolling in the sense that the sizes and shapes of grains and subgrains do not change much as rolling proceeds from pass to pass. As the subgrain boundaries are made from dislocations, the steady state subgrain structure means a steady state dislocation structure.

[1] Note that w_N and d_N do not depend on the plane of observation (T or R) as it should be the case.

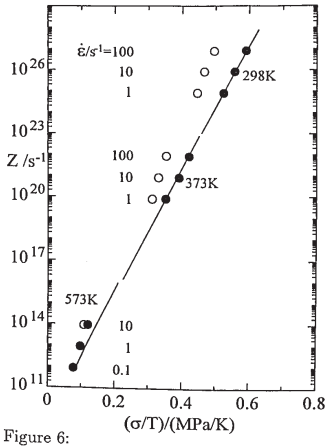

Figure 6:
Relation between $Z = \dot{\epsilon}\,\exp(Q/(k_B T))$ and σ/T ($Q = 142$ kJ/mol). Open symbols: measured at $\epsilon \approx 0.69$, full symbols: steady state.

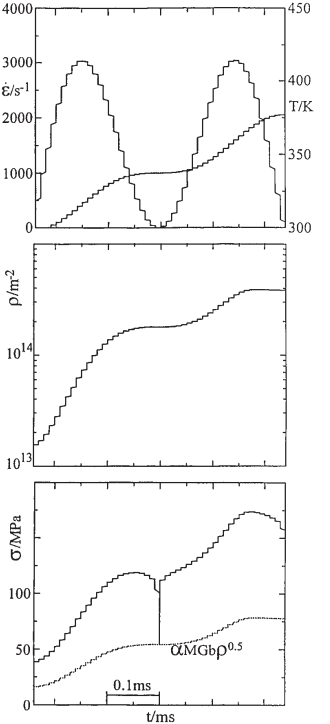

Figure 7: Modeled variation of $\dot{\epsilon}$, T, ρ, and σ as a function of time t in the first rolling pass. $\dot{\epsilon}$ has two maxima as the material enters and leaves the rolls [8]; the average value equals the experimental value $\bar{\dot{\epsilon}}$ (= rolling strain per time for pass). T is assumed to increase linearly with strain ϵ from room temperature to the estimated final temperature $T_H + 30$ K (T_H: typical maximum temperature of the coil after rolling).

The deformation behavior during rolling has been modeled with a simple model using the overall dislocation density ρ as single microstructural parameter in the equations for deformation kinetics and structure evolution. At this stage of work the aim of modeling is to illustrate what may happen during rolling; the model has not been optimized and therefore is not suited for reliable quantitative estimates and conclusions. The equations for deformation kinetics are based on thermally activated glide:

$$\dot{\gamma} = M\,\dot{\epsilon} = b\,\rho\,v, \quad v = v_0\,\exp\left(-\frac{Q}{k_B T}\right)\,\sinh\left(\frac{b\,\Delta a^*\,\tau^*}{k_B T}\right), \quad \Delta a^* = 0.75\,b\,\left(\frac{G\,b}{\rho\,\tau^*}\right)^{1/3} \tag{2}$$

$$\tau^* = \tau - \alpha\,G\,b\sqrt{\rho}, \qquad \tau = \sigma/M \tag{3}$$

($\dot{\gamma}$: shear strain rate, v: dislocation velocity, Δa^*: activation area, τ^*: effective resolved shear stress, τ: applied resolved shear stress, $Q = 142$ kJ/mol, k_B: Boltzmann constant,

$v_0 = 3\times10^5\,\mathrm{m/s}$, $\alpha = 0.19$, Taylor factor $M = 3$). The equations for structure evolution were chosen as:

$$\dot\rho = \dot\rho^+ - \dot\rho^-, \qquad \dot\rho^+ = \frac{2}{bc}\rho^{0.5}\dot\gamma, \qquad \dot\rho^- = A^-\,\rho\,\frac{\tau}{G(T)}\,\exp\left(-\frac{Q}{k_BT}\right)\,\sinh\left(\frac{V\tau}{k_BT}\right) \quad (4)$$

($\dot\rho^+$: dislocation generation rate, $\dot\rho^-$: dislocation annihilation rate, $c = 445$, $A^- = 3.2\times10^{13}/\mathrm{s}$, $V = 115\,b^3$). The $\dot\rho^-$-expression was chosen so that experimental data for the steady state Z-σ-relation obtained from (4) is in accord with the experimental results (Fig. 6).

The set of equations (2), (3) and (4) forms a system of coupled differential equations which can be solved for each pass of rolling. Fig. 7 shows the assumed variation of $\dot\epsilon$ and T during the first pass and the resulting variation of flow stress τ and dislocation density ρ. With the chosen values of c and initial dislocation density (consistent with initial flow stress), ρ saturates already in the first pass. Similarly, σ reaches a plateau. In the subsequent passes the levels of ρ and σ change only slightly in consequence of the limited changes of $\bar{\dot\epsilon}$ and T_H (see Fig. 5). This is displayed in Fig. 8. It appears noteworthy that the model predicts slight softening of the material during passage of the roll; this is a consequence of the assumed increase in T. In the present state the model predicts a rather large athermal stress component $\alpha\,M\,b\,G\,\sqrt{\rho}$ which is also shown in Figs. 7 and 8; its magnitude depends on the choice of v_0 and α.

This quasi steady state situation corresponds to the limited variation of the subgrain size w_{UN} measured in the rolling plane (Fig. 5). The subgrain sizes w_{UN} and w_{RT} allow an estimate of the normalized flow stress σ/G at the ends of the passes as $18\,b\,G/\sigma$ (relation (1)). The resulting data are in accord with the normalized room temperature flow stress R_m/G of the foils (measured as ultimate tensile strength at a strain of 0.01). This agreement can be rationalized by noting that the steady state flow stress during rolling ($\bar{\dot\epsilon} \approx 10^3/\mathrm{s}$, 400 K) is not too far from the steady state expected in room temperature testing ($\dot\epsilon = 4\times10^{-3}/\mathrm{s}$, 300 K). Thus the R_m-data back the flow stresses obtained from w.

It is seen that the σ/G-values obtained from the simple one-parameter model and from the measured subgrain sizes (in the long subgrain dimension) are in the same order of magnitude. In view of the incertainties and errors involved in determining both types of data the agreement is considered satisfactory and gives confidence in the qualitative validity of simulation. The analysis presented above confirms the idea of saturation of dislocation density by dynamic recovery during rolling of Al foil. However, the dislocation structure is significantly modified by the large angle grain boundaries whose area increases strongly in the course of rolling. The increase comes to an end as the grain thickness d_T shrinks to values lying in the order of the roughness of the grain boundaries produced by their reaction with subgrain boundaries. Then the further decrease of d_T is stopped by concurrent recombination. This process is called geometric dynamic recrystallization [5,4,6]. It was first detected during deformation at high temperature but apparently takes place even during cold rolling. The large angle grain boundaries become so frequent that the bottom and top faces of the subgrains are in fact mostly made up from large angle boundaries rather than small angle boundaries at a strain of 4.7 when the foil thickness has been brought down to 6.5 μm (Fig. 3). However, there is no indication from microstructural spacings (subgrain size and shape) or tensile tests that the replacement of subgrain by grain boundaries has a significant influence on the steady state flow stress. This is in agreement with previous findings for geometric dynamic recovery [9].

CONCLUSIONS

1. During foil rolling of pure Al (AA1050) the grain structure reaches a quasi steady state by dynamic recovery and geometric dynamic recrystallization with flat subgrains of equiaxed cross section and about 0.9 μm diameter and about 0.45 μm thickness in flat grains of 1 μm

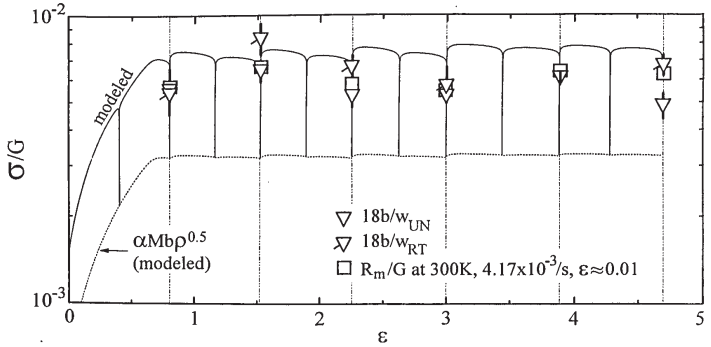

Figure 8: Modeled variation of G-normalized flow stress with rolling strain. Vertical lines mark ends of passes. Triangles: σ/G calculated from w via (1). Squares: normalized ultimate tensile strengths R_m/G of foils.

thickness.

2. A simple model of deformation using the overall dislocation density as single microstructural parameter in the differential equations for deformation kinetics and structure evolution is consistent with the measured steady state $\dot{\epsilon}$-σ-T-relation determined in uniaxial compression.

3. The modeled variation of flow stress during rolling is consistent with the measured variation of subgrain size in the long subgrain dimension.

ACKNOWLEDGMENTS

This work was supported by fellowships of the German Academic Exchange Service (H. A.) and the state of Bavaria (J. K.).

REFERENCES

[1] H. Abral, P. Schlund, H. G. Sockel and W. Blum: Practical Metallography, 34(1998).
[2] A. Voigt: Dr.-Ing. thesis, Universität Erlangen-Nürnberg, 1996.
[3] J. A. Sæter and E. Nes: Mater. Sci. For., 217-222(1996), 447.
[4] H. J. McQueen and W. Blum: this conference.
[5] F. J. Humphreys and M. Hatherly: Recrystallization and Related Annealing Phenomena. Elsevier Science, Oxford, 1995.
[6] W. Blum, Q. Zhu, R. Merkel and H. J. McQueen: Z. Metallkde., 87(1996), 14.
[7] H. J. Frost and M. F. Ashby: Deformation-Mechanism Maps, Pergamon Press, Oxford, 1982.
[8] N. A. Fleck and K. L. Johnson: Int. J. Mech. Sci., 29(1987), 507.
[9] H. J. McQueen, O. Knustad, N. Ryum and J. K. Solberg: Scripta metall., 19(1985), 73.